

Impact of Optical Parametric Amplification Phase on Laser Pulse Compression

Senior Thesis

Jonathan Musgrave

Supervised By:
Dr. Jake Bromage



Institute of Optics
University of Rochester
Spring 2021

Contents

1	Abstract	2
2	Introduction	3
3	Plane Wave Analysis of Non-Collinear Optical Parametric Amplification	3
3.1	Intensity Solutions to Coupled Wave Equation	4
3.2	Phase Solutions to Coupled Wave Equation	5
3.3	Non-Collinear Phase-matching and Walk off versus Non-Walk off Compensated Ge- ometry	6
3.4	Optical Parametric Phase-Sensitivity to Alignment	8
3.5	Approximation of the Compressed Electric field	8
4	Discussion of Phase-Sensitivity Expression's with Numerical Examples	9
4.1	Alignment errors and Compression	10
4.2	Wavefront Angular Aberrations and Compression	11
4.3	Wavefront Spatial Aberrations and Focusing	13
4.4	Influence of Material Properties on System Sensitivity	15
5	Approximations and Assumptions	17
5.1	Other Nonlinear Interactions and Parasitic Effects	17
5.2	Plane Wave Analysis	18
5.3	Temporal and Spatial Walk Off	18
6	Concluding Remarks	19
7	Acknowledgments	19

1 Abstract

Optical Parametric Chirp Pulse Amplification (OPCPA) is an intensely researched topic and has gained a lot of traction in the past 25 years for the continued development of ultrashort pulse generation. A precise control and knowledge of a systems spectral and spatial phase is required for Fourier transform-limited pulse compression. Specifically, during parametric amplification a nonlinear phase accumulation can be detrimental to the peak power and pulse width of a system after compression. In this article plane wave analysis of OPA will be used in order to study the influence of material, wavefront, and optical alignment on spectral and spatial phase, in relevance to recompression and focusing of OPCPA systems. Expressions for pump-angle and signal-angle sensitivity is derived that can be used to evaluate an OPCPA systems resilience to spatial and spectral aberration as well as misalignment. These expressions are used to evaluate the tolerance of OPCPA systems that utilize partially deuterated potassium dihydrogen phosphate (DKDP) with a gain-bandwidth in the visible spectrum. Wavefront data collected at the Laser Laboratory for Energetics' (LLE) on the MTW-OPAL system is used to apply these expression in context to recompression and focusing of amplified ultrashort pulses. We show a resiliency to phase accumulation in the presence of both wavefront aberration of the signal and pump as well as high resiliency to alignment error for non-walk off and walk off compensated geometries. The peak power of OPCPA systems of this type are therefore limited more drastically by the signal gain rather than phase accumulation.

2 Introduction

Optical parametric amplification (OPA) was demonstrated very soon after the advent of the laser and advances in OPAs have been closely related to the broader trends of laser technology development.¹ The development of theory and application of OPA schemes has been pursued as a promising platform for broadband amplification schemes. The nonlinear three wave mixing process highly depends on the phase-matching condition between the pump, signal, and idler photons. Optimal energy transfer from the pump beam to the signal and idler beam requires perfect phase-matching of the input waves. Complete energy transfer can be observed under such condition with an optimized crystal length and a sufficiently strong pump intensity. The spectral extent of optimal phase-matching for a signal beam can be extended by adjusting the wave-vectors to a non-collinear geometry.

Non-collinear Optical Parametric Amplifiers (NOPA) plays a key role in many laser applications. Their ability to offer both high gain and high-gain bandwidth have provided a versatile platform for generating extremely tunable coherent light sources. NOPA has provided a promising platform for generation of peak petawatt laser pulses. NOPA has also allowed amplification in spectral regimes that traditional solid-state laser amplifiers cannot reach. Applications of NOPA to amplify chirped pulses is not a surprising jump. The basic principles of OPCPA is to amplify a linearly chirped signal pulse over a large bandwidth by conversion of a highly energetic and narrow bandwidth pump pulse. The high gain bandwidth offered by NOPA systems permit convenient ultrashort pulse amplification and has demonstrated generation of amplification of few cycle optical pulses.²⁻⁴

However, at these extremes it becomes increasingly important to analyze the physical process of NOPA in detail. The nonlinear parametric process has been studied intensely both analytically and numerically.⁵ When discussing the compression of chirped pulses, it is extremely important to analyze the spectral phase accumulation during amplification. Previous work has been conducted studying the optimization of such systems.⁶ This paper presents a numeric and analytic analysis of the following topics:

1. The influence of angular misalignment on residual OPA signal phase
2. The signal phase-sensitivity to aberrations present in the signal and/or pump wavefront.
3. The analysis of residual spectral phase on compression for amplified signal pulses.
4. The analysis of residual spatial phase on focusing for amplified signal pulses.
5. The influence of material dispersion on non-collinearity and the implications on phase-sensitivity.

The primary analytic tool is an expression derived by Ross *et al.*⁶ based on a formulation constructed by Armstrong *et al.*⁷ which provides a useful and insightful analysis despite the inherent approximations. The model of particular interest in this article is a broadband type 1 OPCPA system using a monochromatic 526.5nm laser to pump a DKDP crystal. Deuterations of different levels Ranging from 70% to 100% are considered to analyze different degrees of non-collinearity and material dispersion.

3 Plane Wave Analysis of Non-Collinear Optical Parametric Amplification

The work done in Armstrong *et al.*⁷ is based on plane wave solutions of the coupled wave equations taking advantage of both the slowly varying envelope approximation and lossless medium.

The solutions produced by Armstrong provide an analytic analysis tool for both the amplitude and phase of the signal pulse through propagation. These solutions were extended in Ross *et al.*⁶ to discuss the amplification of chirped pulses with geometries that closely match the group velocities between the signal and idler pulses, for which the highest bandwidth is generated. This is the situation with which we are primarily concerned. The solutions presented in Ross *et al.* are valid to first order and do not take into account higher order dispersion effects such as group velocity dispersion (GVD) in the signal and idler pulse. Therefore, the limit of accuracy of the following analytic expressions is when the group-delay difference between pump and signal over the length of the crystal becomes a significant fraction of the pulse duration.

The polarization response function to a high-intensity pump wave at frequency ω_p and a less intense signal frequency ω_s in a second-order nonlinear crystal causes both waves to beat together generating a component of the polarization at a third idler frequency ω_i . The interaction between this idler wave and pump generates a component of the polarization that causes the signal frequencies amplitude to grow. Effectively transferring energy from the pump to the signal. The conditions of this three wave mixing process in the photon picture requires the annihilation of a pump photon and simultaneous generation of an idler and signal photon in an elastic process. The limit to this interaction is k-vector matching which is dictated due to a conservation of energy and momentum. This requires the sum of the signal and idler frequency (k-vector) to equal the pump frequency (k-vector) expressed

$$\begin{aligned}\omega_p &= \omega_s + \omega_i, \\ k_p &= k_s + k_i.\end{aligned}$$

Commonly known expressions for the three wave mixing process is a coupled wave equation derived from a plane-wave analysis of the nonlinear wave equation of electromagnetic radiation propagating in a nonlinear medium. Where the change in amplitude of the three waves are written

$$\begin{aligned}\frac{dA_i}{dz} &= -j \frac{\omega_i d_{eff}}{n_i c} A_s^* A_p e^{-j\Delta k z} \\ \frac{dA_s}{dz} &= -j \frac{\omega_s d_{eff}}{n_s c} A_i^* A_p e^{-j\Delta k z} \\ \frac{dA_p}{dz} &= -j \frac{\omega_p d_{eff}}{n_p c} A_s A_i e^{j\Delta k z}\end{aligned}\tag{1}$$

Where d_{eff} is the effective nonlinear coefficient and Δk is the non-collinear phase-matching between the three k-vectors $\Delta \mathbf{k} = \mathbf{k}_p - \mathbf{k}_s - \mathbf{k}_i$. The wave at each frequency is assumed to take the form:

$$\frac{1}{2} A(z) e^{-i(kz - \omega t)} + c.c.$$

The Δk in Eq. (1) is an important parameter to the efficiency of pump to signal energy conversion. Δk 's wavelength and angular dependence drives the main discussion of this paper.

3.1 Intensity Solutions to Coupled Wave Equation

The analytic treatment of this coupled wave equation produces functions for the intensity of the three waves in terms of Jacobi elliptical functions which is valid for any degree of pump and signal initial energy.⁸ The intensity of the pump as the wave propagates is

$$I_p(z) = I_{tot} [b + (f - b) sn^2(\sqrt{(q - b)}g(z + z_0),)].\tag{2}$$

Where intensity is defined $I_r = (1/2)\epsilon_0 n_r c |A_r|^2$ and $r \in i, s, p$. The sinius amplitudinis, $sn(u, m)$, is defined:

$$u = \int_0^{sn(u,m)} dt \frac{1}{\sqrt{(1-t^2)(1-mt^2)}}. \quad (3)$$

The parameters, b, f , and q are dependent initial conditions and are defined in Schimpf *et al.* The elliptic modulus of the sinius amplitudinis, m , is defined:

$$m = \frac{f-b}{q-b} \quad (4)$$

and g is an intensity dependent parameter that is a measure of the strength of the parametric process. g can be expressed

$$g = 4\pi d_{eff} \sqrt{\frac{I_{0p}}{2\epsilon_0 c n_s n_p n_i \lambda_i \lambda_s}}. \quad (5)$$

The solutions for the signal and idler intensities can then be obtained through the Manley-Rowe relations as

$$\begin{aligned} I_i(z) &= I_i(0) + \frac{\omega_i}{\omega_p} [I_p(0) - I_p(z)] \\ I_s(z) &= I_s(0) + \frac{\omega_s}{\omega_p} [I_p(0) - I_p(z)] \end{aligned} \quad (6)$$

The gain of the signal is therefore defined

$$G = \frac{I_s(z)}{I_s(0)} = \frac{\omega_s}{\omega_p} \frac{[I_p(0) - I_p(z)]}{I_s(0)} + 1 \quad (7)$$

3.2 Phase Solutions to Coupled Wave Equation

The solutions for phase of the coupled wave equation comes from solving the imaginary parts of the coupled wave equation and can be expressed as:⁷

$$\begin{aligned} \frac{d\phi_s}{dz} &= -K \frac{\omega_s^2}{k_s} \frac{a_p a_i}{a_s} \cos(\theta) \\ \frac{d\phi_i}{dz} &= -K \frac{\omega_i^2}{k_i} \frac{a_p a_s}{a_i} \cos(\theta) \\ \frac{d\phi_p}{dz} &= -K \frac{\omega_p^2}{k_p} \frac{a_s a_i}{a_p} \cos(\theta) \end{aligned} \quad (8)$$

Where $K = (2\pi/c^2)d_{eff}$. The amplitude of each wave has been expressed as $a e^{i\phi}$ and $\theta = \Delta k z + \phi_p(z) - \phi_s(z) - \phi_i(z)$. The solutions are readily combined and integrated and by assuming zero initial idler photons (the situation we are concerned with in an OPCPA system) it can be shown, after a considerable amount of algebra and calculus, the expression for the OPA phase as a function of frequency and propagation length takes the form⁶

$$\begin{aligned} \phi_s(\omega, z) &= \phi_s(0) - \frac{\Delta k(\omega)z}{2} + \frac{\Delta k(\omega)\gamma_s^2}{2} \int_0^z \frac{dz}{f + \gamma_s^2} \\ \phi_i(\omega, z) &= \phi_p(0) - \phi_s(0) - \frac{\pi}{2} - \frac{\Delta k(\omega)z}{2} \\ \phi_p(\omega, z) &= \phi_p(0) - \frac{\Delta k(\omega)}{2} \int_0^z \frac{f dz}{1-f}, \end{aligned} \quad (9)$$

where $f = 1 - I_p/I_p(0)$ and is the fractional depletion of the pump beam. The gamma terms depend on initial conditions of input intensities.

$$\gamma_s^2 = \frac{\omega_p I_s(0)}{\omega_s I_p(0)}, \gamma_i^2 = \frac{\omega_p I_i(0)}{\omega_i I_p(0)}. \quad (10)$$

A further simplification for the signal's phase can be made when the pump's depletion through propagation is very small, the so-called 'small-signal gain' regime. The solution for this approximation takes the form of Eq. (11),

$$\phi_s = \phi_s(0) - \frac{\Delta k z}{2} + \tan^{-1} \left[\frac{\Delta k}{2\sqrt{g^2 - (\frac{\Delta k}{2})^2}} \tanh(\sqrt{g^2 - (\frac{\Delta k}{2})^2} z) \right]. \quad (11)$$

A consequence of Eq. (9) is that when there is perfect phase-matching ($\Delta k = 0$) there is no phase accumulation in the signal and is the ideal situation for pulse compression.

3.3 Non-Collinear Phase-matching and Walk off versus Non-Walk off Compensated Geometry

As discussed above, phase-matching is necessary for efficient energy transfer from the pump pulse to the signal pulse. Broadband phase-matching can be accomplished by matching the group velocity of the signal and idler pulses.⁵ In practice birefringent materials must be used in order to fulfill broad-bandwidth phase-matching and for Type-I phase-matching, the situation we will investigate, the pump beam is used in an extraordinary polarization state with the signal and idler beams in the ordinary polarization state. Non-collinear geometry of the three waves is utilized for the broadest possible gain bandwidth.

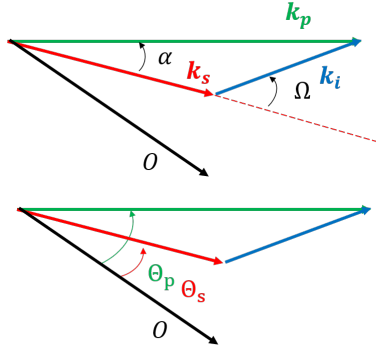


Figure 1: Phase-matching between the wave vectors of the three beams. O is the optical axis of the nonlinear crystal

The vector sum ($\Delta \mathbf{k}$) can be split into its transverse and longitudinal scalar components relative to the signal vector

$$\begin{aligned} \Delta k_{\parallel} &= k_p \cos(\alpha) - k_s - k_i \cos(\Omega), \\ \Delta k_{\perp} &= k_p \sin(\alpha) - k_i \sin(\Omega). \end{aligned} \quad (12)$$

Where α is the angle between the pump and signal and is referred to as the pump tilt angle expressed $\alpha = \Theta_p - \Theta_s$. Ω is the resulting angle between idler and signal. The geometry is illustrated in

Fig. 1. Assuming the longitudinal component is much larger than the transverse component of the phase-mismatch a scalar form of the phase-matching equation can be expressed⁸

$$\Delta k = k_p \cos(\alpha) - k_s - \sqrt{k_p^2 \cos(\alpha)^2 - k_p^2 + k_i^2}. \quad (13)$$

In practice the k_s dependence on wavelength restricts perfect phase-matching, $\Delta k = 0$, to specific wavelengths. Therefore we observe a net accumulation of spectral phase across the gain-bandwidth that is inherited in OPCPA systems. Ideally that residual phase is compensated in the compression element. A more detailed discussion of this will be addressed in Section 4

The non-collinear angles between the signal and pump cause the two transverse beam profiles to walk off as they propagate. The α values usually do not exceed more than a few degrees and spatial walk off between the two beams are often negligible for beams of sufficient size. However for sufficiently small beams or large pump tilts it is possible to compensate for this effect by choosing a geometry such that the refraction of the pump's Poynting vector partially compensates this non-collinear angle in what is referred to as the walk-off compensated (WC) geometry. Every NOPA system has two operational non-collinear geometries that produce the same gain bandwidth and phase accumulation (see Fig. 2). Which geometry is chosen depends on several factors.??

One consideration is the sensitivity of phase-mismatch to angular misalignment of the pump or signal. In the non-walk-off compensated (NWC) geometry the Θ dependence of the pump wave refractive index compensates for a deviation in optimal α angle. Meaning the k -vector and cosine term in Eq. (13) are inversely proportional. In the WC geometry the values become proportional and the nominal phase-mismatch, and therefore gain, will be much more sensitive to angular deviation. These effects are shown in Fig. (2) for both cases, WC and NWC. The higher sensitivity for the WC case results in a narrower gain distribution when plotted versus the pump angle as compared to the NWC case.

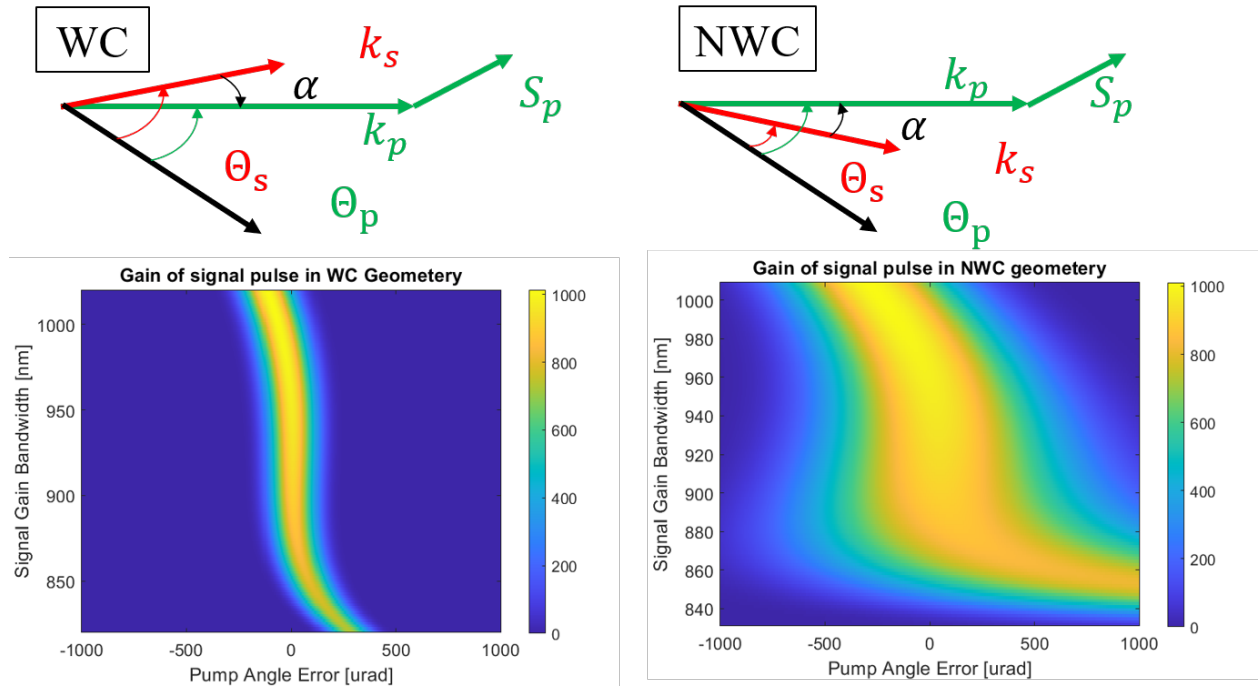


Figure 2: Walk off compensated (WC) and non-walk-off compensated (NWC) geometries of OPA and the corresponding gain across the bandwidth as a function of pump angle error

3.4 Optical Parametric Phase-Sensitivity to Alignment

Starting from Eq. (9) the phase sensitivity of the signal can be expressed as a derivative with respect to a change in either the pump or signal angle, where $r \in p, s$ for pump and signal respectively,

$$\frac{\delta\phi_s}{\delta\Theta_r} = \frac{1}{2} \frac{\delta\Delta k}{\delta\Theta_r} \left(-z + \int_0^z \frac{\gamma_s^2}{f + \gamma_s^2} dz \right). \quad (14)$$

In the small-signal gain limit we find Eq.(14) can be approximated as:

$$\frac{\delta\phi_s}{\delta\Theta_r} = \frac{1}{2} \frac{\delta\Delta k}{\delta\Theta_r} \left(-z + \frac{\Gamma^2 \tanh(z\Gamma) - \Gamma(\frac{\Delta k}{2})^2 z \operatorname{sech}(z\Gamma)^2 + (\frac{\Delta k}{2})^2 \tanh(z\Gamma)}{\Gamma^3 + \Gamma(\frac{\Delta k}{2})^2 \tanh(z\Gamma)} \right). \quad (15)$$

$\Gamma = \sqrt{g^2 - (\frac{\Delta k}{2})^2}$ and approaches g as the phase-mismatch approaches zero. Analysis of this equation shows a proportional relationship between the phase-mismatch sensitivity to angular aberration. Using the definition of phase-mismatch previously stated (Eq. 13) we can then show that the phase-mismatch sensitivity to a signal angle is

$$\frac{\delta\Delta k}{\delta\Theta_s} = -k_p \sin(\alpha) + \left(\frac{k_p^2 \sin(\alpha) \cos(\alpha)}{\sqrt{k_p^2 \cos(\alpha)^2 - k_p^2 + k_i^2}} \right). \quad (16)$$

A similar analysis shows the phase-mismatch sensitivity to pump angle is defined as

$$\frac{\delta\Delta k}{\delta\Theta_p} = \frac{dk_p}{d\Theta_p} \cos(\alpha) - k_p \sin(\alpha) \left(1 - \frac{\frac{dk_p}{d\Theta_p} \sin(\alpha) + k_p \cos(\alpha)}{\sqrt{k_p^2 \cos(\alpha)^2 - k_p^2 + k_i^2}} \right) \quad (17)$$

The derivative of pump k-vector with respect to angle in general can be solved analytically. For OPCPA with DKDP crystals, the pump's index of refraction can be modeled:⁹

$$n_p(\Theta) = \sqrt{(1-x)n_K(\Theta)^2 + xn_D(\Theta)}, \quad (18)$$

where x is the fractional amount of deuteration and $x = 1$ corresponds to a 100% exchange of hydrogen for deuterium. n_K and n_D is the respective index of refraction for pure KDP and pure DKDP respectively. The pumps k-vector sensitivity can then be written

$$\frac{dk_p}{d\Theta_p} = \frac{\omega_p}{c} \frac{\cos(\Theta_p) \sin(\Theta_p)}{n_p(\Theta_p)} \left((1-x)n_K^4 \frac{n_{Ke}^2 - n_{Ko}^2}{n_{Ke}^2 n_{Ko}^2} + x \frac{n_{De}^2 - n_{Do}^2}{n_{De}^2 n_{Do}^2} \right). \quad (19)$$

Where the subscript e and o refer to the extraordinary and ordinary refractive indices, respectively. Further analysis of these expressions will be discussed in the following sections.

3.5 Approximation of the Compressed Electric field

The use of dispersive elements for precise control of spectral phase in OPCPA and ultrafast optics has been highly studied and developed.¹⁰ The principle is to compensate the chirp introduced to the signal beam from the stretching component (ϕ_s^S) as well as the spectral phase accumulation in the amplifier (ϕ_s^A) with a compression element (ϕ_s^C) such that $\Delta\phi = \phi_s^C - \phi_s^A - \phi_s^S = 0$. The output electric field in the frequency domain is

$$E(\omega) = \sqrt{G(\omega)S(\omega)} \exp(i\Delta\phi) \quad (20)$$

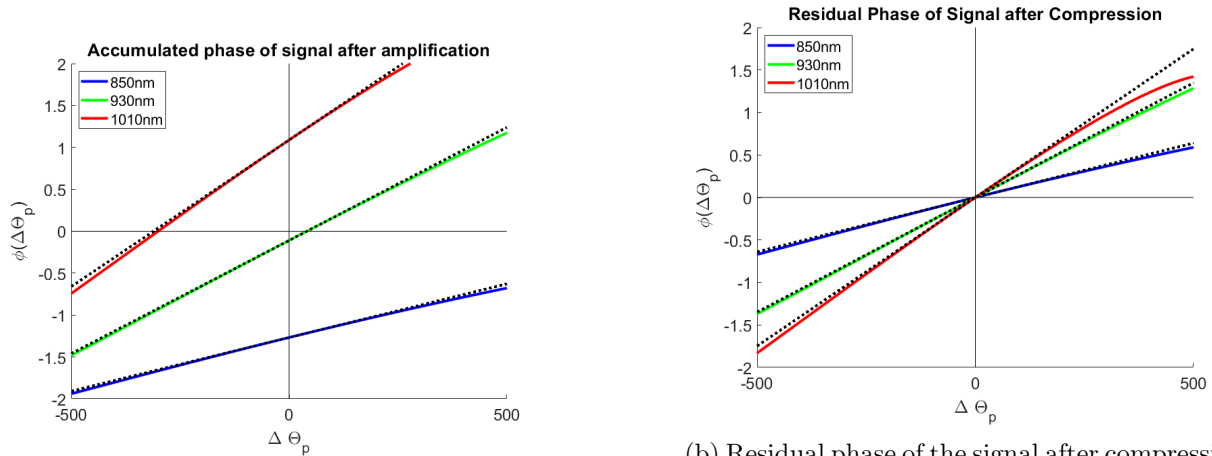
where the G is the gain of the OPA and S is the input spectral function. In the nominal system design we can assume that $\Delta\phi = 0$. However, this relationship does not hold in the presence of angular deviation of the signal or pump beam. We will refer to the nominal design spectral phase accumulated during the OPA as $\phi_s^0(\Theta_0)$. If we expand the spectral phase of the OPA in a two-dimensional Taylor series around the nominal design we find

$$\phi_s(\omega, \Theta_p, \Theta_s) = \phi_s^0 + \frac{\delta\phi_s}{\delta\Theta_p} \Delta\Theta_p + \frac{\delta\phi_s}{\delta\Theta_s} \Delta\Theta_s + \frac{1}{2} \frac{\delta^2\phi_s}{\delta\Theta_p^2} \Delta\Theta_p^2 + \frac{\delta^2\phi_s}{\delta\Theta_p\delta\Theta_s} \Delta\Theta_s\Delta\Theta_p + \frac{1}{2} \frac{\delta^2\phi_s}{\delta\Theta_s^2} \Delta\Theta_s^2 \dots \quad (21)$$

Note that it is not explicitly shown but the derivatives are evaluated at the nominal design (Θ_0). Truncating the Taylor polynomial to a linear approximation (i.e. removing the higher order terms) provides a high accuracy fit to the phase function in the region of non-trivial gain. This fit is shown in one dimension (deviated pump angle) in figure 3. If we assume in our nominal design we are able to correct for all of the systems residual phase accumulated through amplification ($\Delta\phi = 0$). The electric field after compression can then be expressed as a function of the phase-sensitivity to the pump and/or signal angle:

$$E(\omega, \Theta_p, \Theta_s) = \sqrt{GS} \exp\left(i \frac{\delta\phi_s}{\delta\Theta_p} \Delta\Theta_p\right) \exp\left(i \frac{\delta\phi_s}{\delta\Theta_s} \Delta\Theta_s\right). \quad (22)$$

This allows for computationally efficient calculations of frequency domain electric field at the output of an OPCPA system while also providing a tool to evaluate the resiliency to angular aberration of any system by calculating values only related to the nominal system.



(a) Accumulated phase of the signal after amplification

(b) Residual phase of the signal after compression assuming all nominal phase (ϕ_s^0) is corrected from the compression element

Figure 3: Linear Approximation of the spectral phase as a function of deviated pump angle computed numerically (solid lines) and approximated linearly using phase sensitivity expression (dashed lines)

4 Discussion of Phase-Sensitivity Expression's with Numerical Examples

An analysis of OPCPA sensitivity to angles will be discussed in the following section. We will discuss how optical alignment, wavefront aberration, and material affect the spatial and spectral

phase of the signal wavefront with relevance to pulse compression and focusing using numerical calculations. The examples will illustrate type-1 phase-matching OPCPA for a DKDP crystal operated with a $526.5nm$ narrow bandwidth pump. To follow the design of the MTW-OPAL final NOPA, we model our beams as $45x45mm$ square flat "top hat" profiles in both longitudinal and transverse dimension modeled with a 10th order super Gaussian. For beams of uniform intensity, an approximation we will make for our system, the intensity and phase of the modeled pulse can be calculated using Eq. (2) and (9) respectively. Approximations ignoring other nonlinear conversions and Poynting vector walk-off were also made and the accuracy of these results are explained in finer detail in Section 5.

A variety of DKDP crystals with differing levels of deuteration will be explored for their corresponding material properties and benefits. The non-collinearity of each system is of particular importance and will depend on the amount of deuteration. A list of the values of the different non-collinear angles for both NWC and WC geometries are presented in Table 1 It is favorable to build systems with high levels of deuteration due to DKDP crystal's being simpler to manufacture to large size.

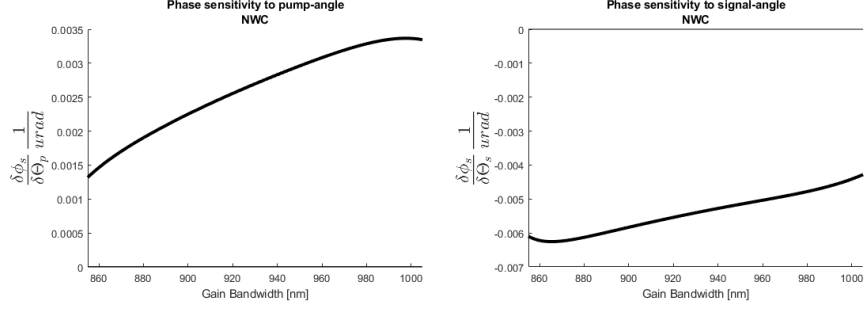
Table 1: Non-collinear angles for optimal phase-matching rounded to two significant digits. In conversion between the NWC and WC geometry the pump angle was constant while the signal angle varied, causing changes in α .

Deuteration (%)	$ \alpha $ (deg.)	Θ_p (deg.)	Θ_s (deg.) NWC	Θ_s (deg.) WC
70	0.34	38.08	37.74	38.42
75	0.46	37.90	37.44	38.36
80	0.56	37.72	37.16	38.28
85	0.67	37.56	36.89	38.23
90	0.75	37.38	36.63	38.13
95	0.84	37.22	36.38	38.06
100	0.92	37.05	36.13	37.97

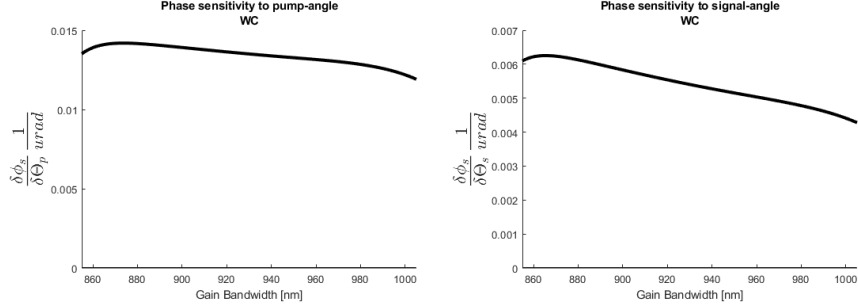
4.1 Alignment errors and Compression

Section 3 addressed the reduction of gain caused by alignment errors for both the WC and NWC geometries. The Following addresses the degradation of peak power NWC geometry with a deuteration level of 90%, which is relevant for NOPA5, the final amplifier in the MTW-OPAL system at the laser Laboratory for Energetics (LLE). For perfection recompression, the spectral phase is constant. The ideal situation, then, is when the phase sensitivity has no slope. That would equate to a wavelength-independent change in phase. In general, this is not the case as seen in our calculated example (Fig. 4).

The linear approximation of the phase error for the electric field at the output of the system causes the uncorrected spectral phase of the system to have the same wavelength dependence as the sensitivity expression. The compressed pulse can then be reconstructed in the time domain. The following will assume only errors present from alignment, ignoring local angular aberrations from the wavefront gradient. Furthermore we assume alignment is within $\pm 250\mu rad$ of nominal, which is straightforward to achieve in practice. The difference in sensitivity across the bandwidth for the NWC and WC is at most only a couple miliradians per micro radian. Meaning the wavelength dependency for these system's under an alignment error is negligible. Peak power at the output will



(a) NWC Phase sensitivity to Signal and pump angle plotted across spectral domain



(b) WC Phase sensitivity to Signal and pump angle plotted across spectral domain

Figure 4: The phase sensitivity of both geometry choices of a 90% Deuterated KDP crystal pumped at 526.5nm

not show strong deviation from nominal (Fig. 5). The limiting consideration, then, in alignment control will be loss of amplifier gain, not spectral phase accumulation.

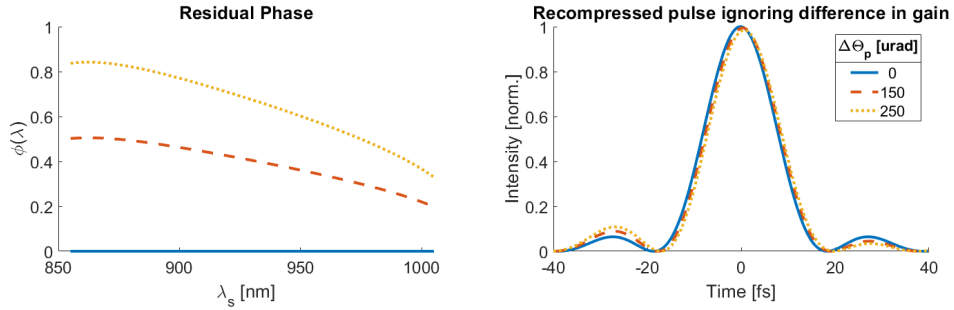


Figure 5: Effect of spectral phase on signal pulse in the presence of misalignment. Assumed perfect planar wavefronts all deviated by the same amount of input angle

4.2 Wavefront Angular Aberrations and Compression

The previous section assumed a perfect planar wavefront, free of aberration. This results in a phase-mismatch function that is independent of time and space, an ideal case that is not achievable in real systems. This section will address the the complexity of spatially aberrated pump and signal beams that evolve through time. This equates to a local angular error of the chirped signal that evolves in frequency as well as spatially.

OPCPA systems are designed to minimize time varying effects as much as possible. However,

experimentally the affects of residual radial group delay, non-normal incidence refraction at the crystal surfaces, and residual angular dispersion cause angular errors that evolve as a function of signal frequency, illustrated in Fig. 6. Measurements of the signal wavefront for the LLE’s NOPA5 show a 0.5-waves of aberration with a dominant spherical term (see Fig. 7)

In the following analysis we assume the signal beam has two-waves of chromatic defocus at the crystal input and the pump beam is perfect. Although a significant simplification and a 5x overestimate of the chromatic errors measured for NOPA5, it demonstrates the fact that spectral phase errors can occur when the system is otherwise well aligned.

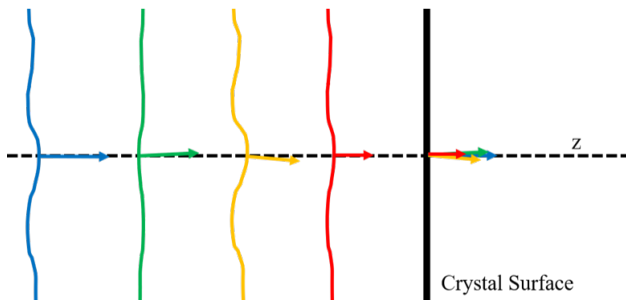


Figure 6: Aberrated signal wavefront as it evolves in space

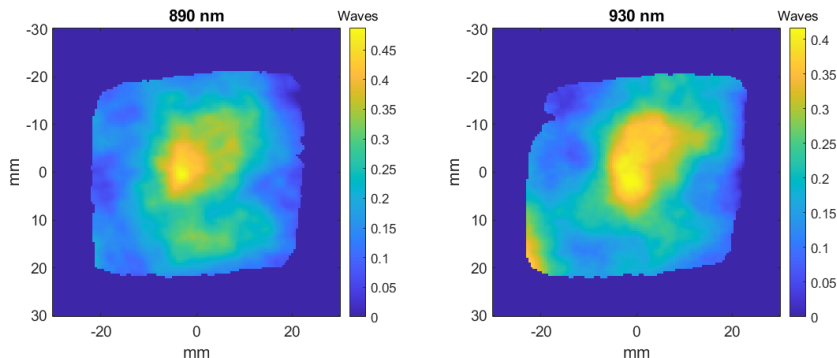
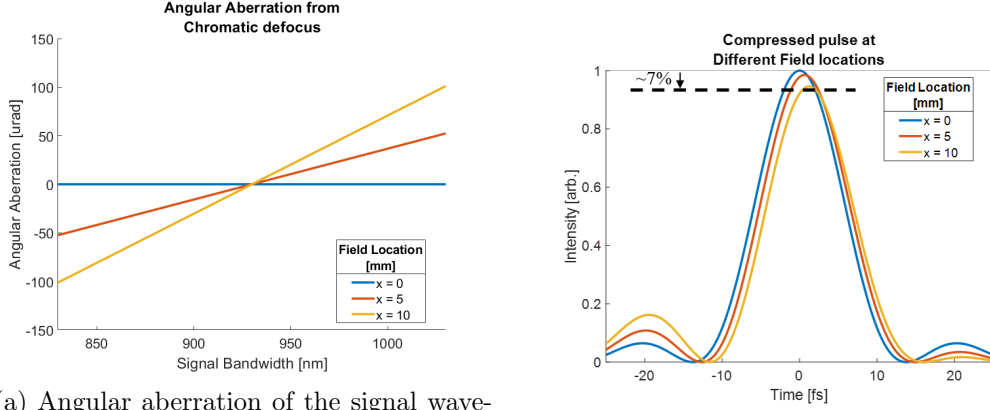


Figure 7: Signal wavefront traces at 890nm and 930nm of the NOPA5 system at LLE courtesy of Dr. Seung-Whan Bahk.

Chromatic defocus is modeled as a parabolic wavefront error that varies linearly with optical frequency. This results in a linear increase in angular aberration across the optical spectrum, with a slope that varies across the beam (see Fig 8). We choose to model the central signal frequency as perfect (0 waves defocus).

The impact of this chromatic defocus illustrates the angle-sensitivity dependence on not only the signal frequency but also on the wavefront correction. In practice large beam diameters are harder to correct over the full field. The evolution of the spatial phase, especially at the beam edge, as a function of frequency will be a more complicated function.



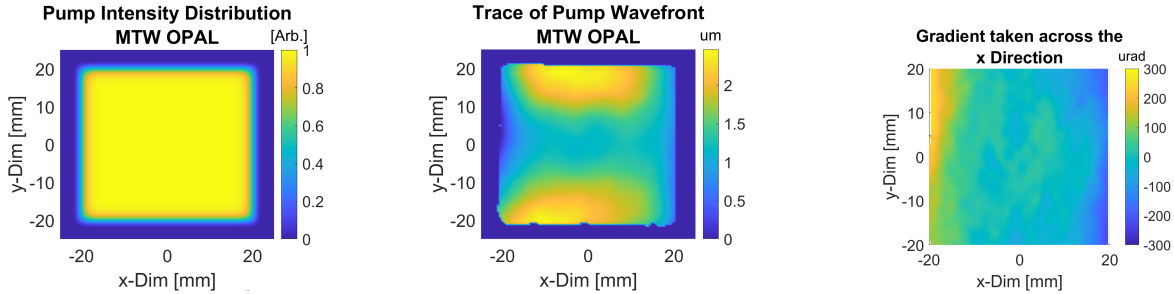
(a) Angular aberration of the signal wavefront across spectrum for different field locations

(b) Compressed pulse at corresponding field locations

Figure 8: The effect of 2-waves chromatic defocus in the signal wavefront on recompression

4.3 Wavefront Spatial Aberrations and Focusing

In the discussion of ultrafast optics phase in all domains is extremely important. Up to now this paper has only discussed the effect of spectral phase in the context of time domain and recompression of the amplified chirp pulse. The phase in the spatial domain is extremely important in the discussion of focusing ultrafast pulses. The following subsection will discuss qualitatively the spatial phase induced on the signal wavefront through amplification and after recompression.



(a) The intensity map modeled with a 10th order super-Gaussian in x and y.

(b) MTW-OPAL wavefront data, courtesy of Dr. Seung-Whan Bahk

(c) Gradient of MTW-OPAL wavefront calculated in the x-direction.

Figure 9: The wavefront captured from MTW-OPAL used in calculating the spatial phase accumulated through amplification.

We again assume that the nominal design of our system corrects for all the accumulated phase during amplification and is able to return an aberration free chirp pulse to a transform-limited Gaussian. Wavefront data collected from the LLE’s MTW-OPAL system shows an astigmatism (Fig. 9b). The intensity distribution of the pump and signal is modeled as a 10th order super-Gaussian. We will again analyze the results of amplification through a 90% deuterized KDP crystal pumped with a monochromatic pump at $526.5nm$ with a gain bandwidth of $200nm$ (FWHM) centered at $930nm$. For simplicity we only assume an aberrated pump wavefront that does not vary with time, and therefore is constant for all signal wavelengths.

The pump wavefront gradient shows, in the extremes, a deviation of approximately $\pm 300\mu rad$

(Fig. 9c). We take the gradient in the direction that has a more drastic wavefront deviation as our non-collinear plane. Using our pump-wavefront angular-sensitivity expression we find that the spatial aberration of the signal can vary above half a radian across the wavefront (Fig. 10). A consequence of our sensitivity function is a near linear relationship between accumulated phase and signal wavelength.

Assuming a perfect focusing system with a focal length arbitrarily chosen to 150mm we can compute the best theoretical focal spot obtainable for our amplified ultrashort pulse as would be measured by a square-law device like a CCD camera. The incoherent addition of the focused spots at each wavelength are amplitude normalized and weighted by the spectrum. We compare the computed focal spot to perfect case where there are no wavefront errors (see Fig. 11). Strehl ratios above 0.97 are obtainable, well above what is considered "diffraction limited", in this specific case of aberrated pump beam and a perfect signal.

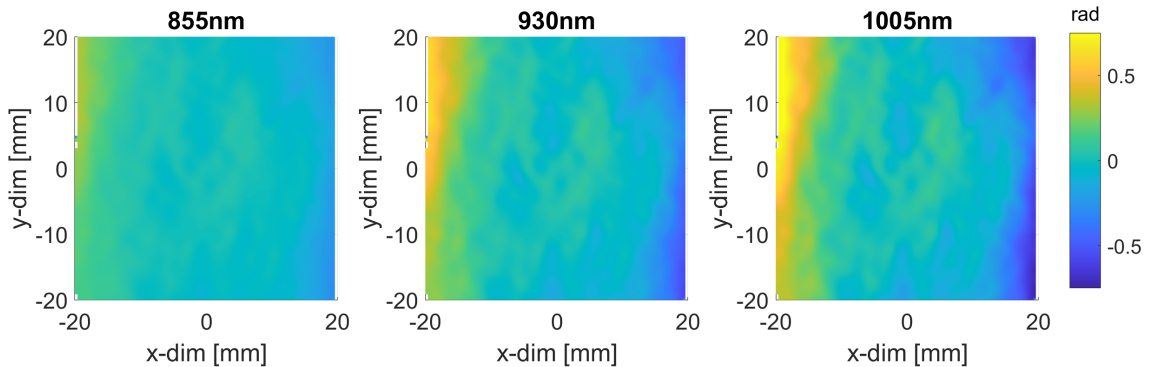


Figure 10: Signal spatial wavefronts at three different wavelengths after compression element.

Therefore the signal wavefront and focusing optics will most likely be the limiting factors for signal focusing rather than the spatial aberrations of the pump. It is interesting to note the astigmatism in the pump wavefront translates to a phase ramp spatially which causes a minor tilt in the focal spot of the focused pulse. Future work could extend this analysis to include the effects of specific aberrations on the focused spot. More analysis could also be conducted that is relevant for field dependent characterization where spectral dependent transverse phase errors may result in significant spatiotemporal aberrations.¹¹

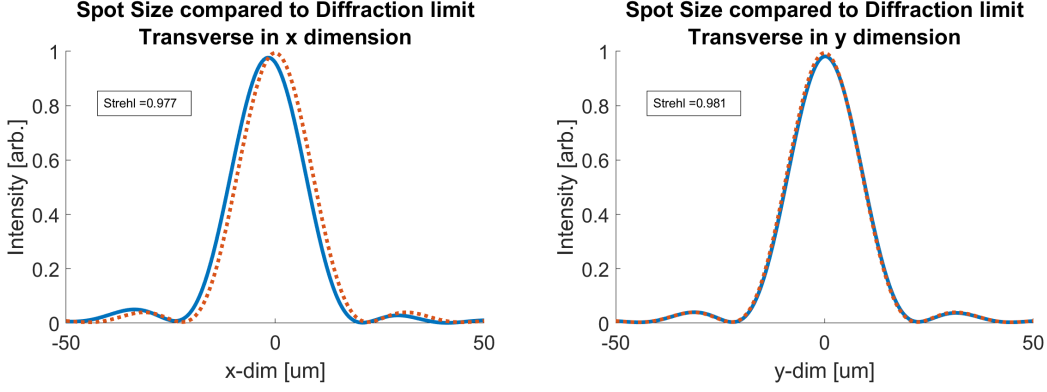


Figure 11: Diffraction limited spot size compared to computed focus. Imaged through perfect system with 150mm focal length. Strehl ratios for each dimension displayed in subplots

4.4 Influence of Material Properties on System Sensitivity

The system sensitivity to both errors in the pump and signal error from alignment and/or wavefront has a strong dependence on the non-collinear angle (α). α is chosen for particular systems in order to optimize the bandwidth of gain. The condition for perfect phase-matching is dependent on a matching of the signal's group velocity projection on the signal idler's group velocity. The condition for ultra-broadband phase-matching can be expressed as a second derivative of the parallel and perpendicular components (Eq. 12) and setting it equal to zero.⁸ The condition is

$$\cos(\Omega_{magic}) = \frac{k_i \left(\frac{\delta\Omega}{\delta\omega_s} \right)^2 - \left(\frac{\delta^2 k_i}{\delta\omega_s^2} \right)}{\left(\frac{\delta^2 k_s}{\delta\omega_s^2} \right)} \quad (23)$$

$$\frac{\delta\Omega}{\delta\omega_s} = \frac{\delta k_i}{\delta\omega_i} \frac{1}{k_i^2} \frac{k_p \sin(\alpha)}{\sqrt{1 - \left(\frac{k_p \sin(\alpha)}{k_i} \right)^2}} \quad (24)$$

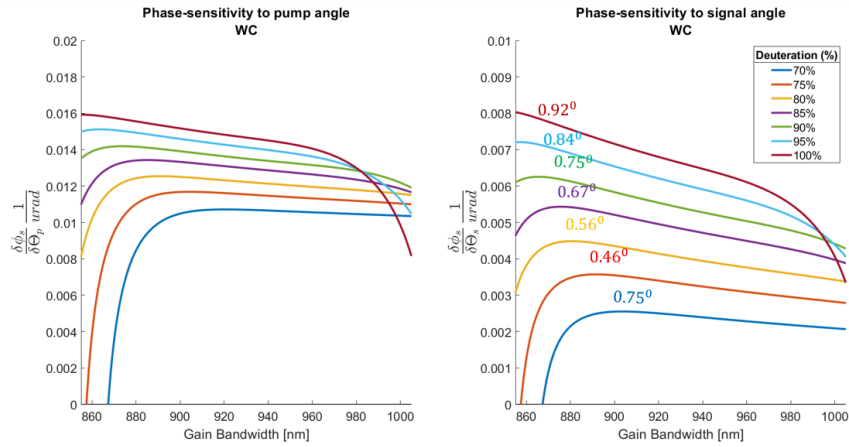
where Ω_{magic} is the ultra-broadband angle and occurs at a specific signal frequency and corresponding non-collinear angle. This corresponds to matching of the angular dispersion of the idler with the group velocity dispersion of the idler. Importantly these are properties of a material described by the analytic Sellmeier formulas. Note that Eq. (23) implies an analytic relationship between the sensitivity equations and material properties due to the proportional relationship between Ω and α .

A consequence of lower fractional deuteration of KDP is an increase in the optimal non-collinear angle (larger Ω_{magic}). This is directly related to our sensitivity functions (Fig. 11). We see in the collinear regime our sensitivity functions approach wavelength independent functions:

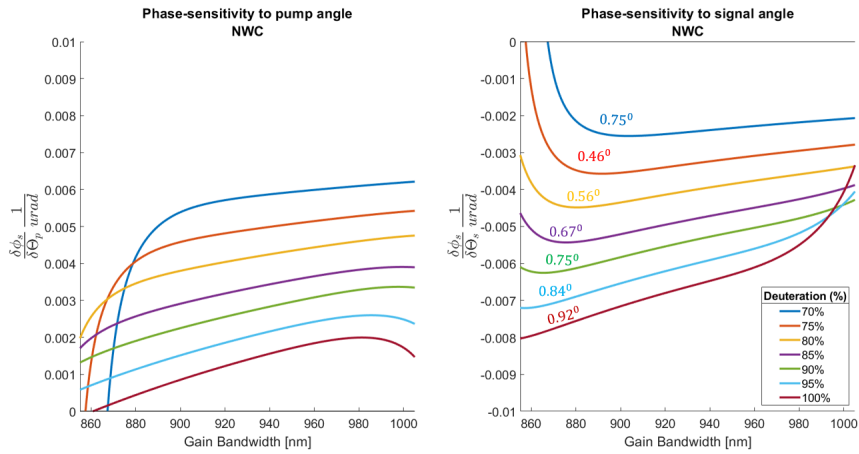
$$\left(\frac{\delta\Delta k}{\delta\Theta_s} \right)_{\alpha=0} = 0 \quad (25)$$

$$\left(\frac{\delta\Delta k}{\delta\Theta_p} \right)_{\alpha=0} = \frac{dk_p}{d\Theta_p}. \quad (26)$$

However, the change in sensitivity is only half of the story. Attention to the change in the gain-bandwidth as a function of the deuteration must also be considered for meaningful analysis on the affect of the fractional deuteration. In general, increased deuteration red-shifts the central



(a) Sensitivity of WC geometry OPA system across bandwidth



(b) Sensitivity of NWC geometry OPA system across bandwidth

Figure 11: Sensitivity function of pump and signal angle for both NWC and WC geometries plotted against bandwidth

amplified signal and decreases the total gain bandwidth in the visible region. This means the high wavelength dependence of the phase-sensitivity function in the sub $900nm$ region for lower deuteration levels is less relevant for recompressing and focusing amplified signal pulses. Phase-sensitivity in general is not strongly dependent on wavelength however does become more meaningful at higher deuteration levels.

The wavelength dependence of OPA phase-sensitivity might not pose a significant problem for DKDP where the system operates in a quasi-collinear regime and for broad bandwidth amplification, α is less than 1° . However, future analysis could be conducted to study other non-collinear OPA systems that have a stronger non-collinear dependence. Second-order nonlinear crystals such as barium borate (BBO) operate with non-collinear angles of a few degrees in magnitude.⁸ It is likely that the wavelength dependence of the phase-sensitivity may be an important issue regarding non-collinearity in these and similar systems.

5 Approximations and Assumptions

In the discussion of numerical simulations based on closed form analytic solutions of the nonlinear wave equation, it is important to recognize the inherent approximations and assumptions that are made in derivation. Moreover, there are a variety of physical phenomena that have been ignored. Parasitic effects such as second harmonic generation (SHG) and other nonlinear effects have not been taken into account in the analysis of this OPA process. The validity and accuracy of the approximations and assumptions is addressed in the following section.

5.1 Other Nonlinear Interactions and Parasitic Effects

This article thus far has largely ignored the effect of the other nonlinear material actions that take place during the propagation of the two input waves. Nonlinear parametric and non-parametric process have been largely studied and the theory for their dynamics well described.¹²

The choice of phase-matching conditions and the large difference between the intensity of pump and signal at the crystal input drives the dominant second-order nonlinear effect to be a difference frequency generation (DFG) of an idler photon. This allows us to largely ignore the effects of sum frequency generation (SFG) at the input of the amplifier where either the pump and signal produce a higher-energy photon. As the signal and idler intensities grow power transfer back to the pump can be seen in a process called re-conversion.

One important parasitic effect for NOPA systems is second-harmonic generation (SHG) of the signal frequency. In the WC geometry for DKDP, the signal is also phase-matched for SHG at certain harmonic frequencies causing notches of low intensity in the spectrum due to the conversion of the signal. Fortunately, the NWC geometry does have the added benefit of operating at a non-collinearity that will not phase-match, at least for DKDP systems, the SHG and this "notching" of the spectrum is not observed. This improves the accuracy of our discussion of NWC geometry systems. However, the parasitic SHG of WC geometry could be studied in future work to investigate the accuracy of the statements made in previous sections.

The discussion of nonlinear effects has been largely focused around the second order ($\chi^{(2)}$) susceptibility of DKDP. The higher order effects ($\chi^{(3)}$ and higher orders) have also been ignored in this analysis. Self focusing of the pump or signal beam can present an issue if the transverse intensity profile is sufficiently non-uniform or nonlinear phase accumulation sufficiently high. The B integral is a measure of the total accumulated nonlinear phase shift and poses a risk for self focusing when above the value 3. We see that at the extremes our pump intensity and crystal length ($1.5GW/cm^2$ and $45mm$ respectively) never exceed a B value inside the nonlinear crystal above 1.4, showing at

these parameters nonlinear phase shifts are a relatively minor might issue that could be explored in future work. Figure 12 shows the calculated B integral of the pump and signal at the output of the crystal, showing a negligible nonlinear phase shift in the signal. Note that these conclusions are consistent with observations made on the MTW-OPAL system. Measurements of the pump beam profiles after the amplifier show no signs of small-scale self focusing at the intensities assumed in these numerical simulations ($1.5\text{GW}/\text{cm}^2$).

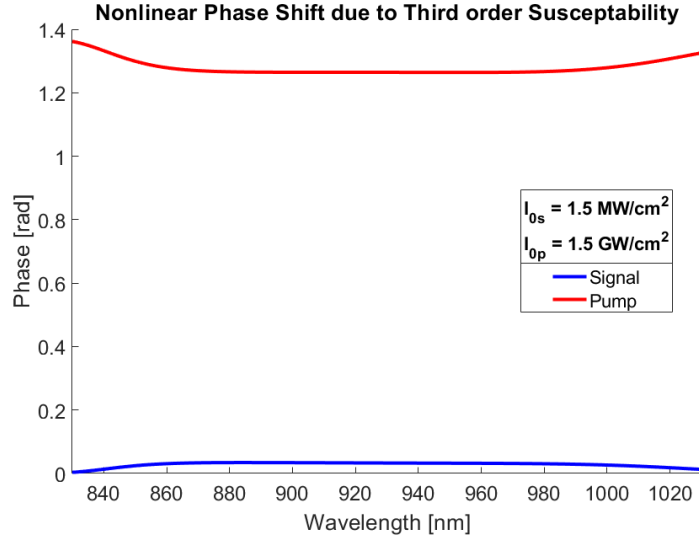


Figure 12: Calculated B-integral for the signal and pump

We have also chosen to ignore all the other higher order terms due to the system operation being far from the phase-matching conditions of the higher order terms.

All interactions described thus far are described parametric process (photon energy conserving). In general non-parametric processes can also occur (Stimulated Raman Scattering for instance) but have also been ignored under the pretext that the frequency and phase shift in general is negligible.

5.2 Plane Wave Analysis

Inherent in any plane wave solutions to the nonlinear wave equation is the assumption of an infinite extent of the wave-front in the transverse direction meaning an infinite amount of power which is physically impossible. Plane wave analysis allows for simplistic and analytic solutions that shed light on the finer details of many physical processes. The analytic solutions are derived from generally accepted solutions⁶ and the accuracy of these solutions will therefore be within the realm of reference [6].

Our numerical simulations have assumed the chirp of the signal at the input face of the crystal is large, as required by nanosecond-pumped OPCPA systems. Therefore, our analysis assumes spatially monochromatic input waves that evolve in time at the crystal input. This, along with sufficient intensity uniformity increases the accuracy of the plane wave analysis

5.3 Temporal and Spatial Walk Off

Spatial walk off was briefly discussed in the plane wave analysis section. The walk off of the pump beam's Poynting vector from the signal beams Poynting vector as they both propagate through the NOPA is of relevance in systems where the ratio of the beam diameter to propagation

length is sufficiently small. The systems modeled in this analysis is able to ignore the spatial walk off between the pump, signal and idler beam because of the large beam diameter ($\approx 45mm$), small non-collinearity angles ($\alpha < 1^\circ$), and short crystal propagation length ($\approx 50mm$).

The temporal slip of the pump from the pump and signal and idler has been assumed to be negligible in this discussion. We have assumed that a particular time slice of the pump maintains the same overlap with a given spectral portion of the signal. An assumption made valid by the fact that in practice, the temporal walk off of the pump is sub-picosecond for crystal widths that are used ($\approx 50mm$). Which is much less than the pump's pulse width of $1.5ns$.

6 Concluding Remarks

The sensitivity expressions derived in this work provide a computationally efficient method for calculating the signal wavefront phase, both for small-signal and high-efficiency amplifiers. We expect these expressions will be used in numerical modeling, optimization, and tolerancing for future OPCPA systems. The linear approximation made for the signal wavefront phase-error has not shown to be inaccurate for the systems we are modeling and we believe it to be accurate in all regions that show non-trivial gain.

The tolerance angular aberrations for optimal signal gain is to extremely tight. In OPCPA control to micro-radians is required for efficient amplification. Therefore the relative resilience of compression and focusing of OPCPA systems to pump and signal aberrations is not entirely surprising. Perhaps a more accurate description of the gain and phase relationship of OPA amplification is that the system constraints on the signal gain dominate constraints on signal-phase. Meaning that for OPCPA, at least in the examples discussed in this paper, non-optimal gain will limit the peak power of the system well before residual-phase limits the compression or focusing of the system.

The discussion of material influence on non-collinearity sheds light on the relationship between NOPA and experimental tolerances. Future work involving an analysis of the mechanism that cause the change in material dispersion on different deuteration would be interesting as well as contributing significantly to the ultrafast optics community, and especially beneficial for systems with large beam diameters such as those at LLE or Lawrence Livermore National Laboratory.

The continued technological development of OPCPA will lead to the next generation of ultrafast lasers. The sensitivity of spectral phase in OPCPA systems discussed in this thesis addresses the effects of non-collinearity on the compression of amplified ultrashort pulses. The high resiliency of the OPA geometry proves the utility for amplification of large-diameter beams with broadband pulses

7 Acknowledgments

I would like to acknowledge and thank all persons that have supported me in my academic pursuits. I want to especially thank Dr. Jake Bromage for his significant support to this thesis both as a mentor and contributor. I would also like to thank Dr. Seung-Whan Bahk for his contribution to the realization of this project. I would also like to acknowledge Dr. Wayne Knox for his work in organizing the senior thesis course as well as introducing and accustoming me to the research environment at the Institute of Optics. Lastly I would like to thank my mother, Dr. Lynn Yanagihara, and my father, Dr. James Musgrave, for their continuous support in my academic career.

References

- [1] A. P. Piskarskas and R. Butkus. “20 Years of Progress in OPCPA”. en. In: *Frontiers in Optics 2012/Laser Science XXVIII*. Rochester, New York: OSA, 2012, FTu1B.1. ISBN: 978-1-55752-956-5. DOI: 10.1364/FIO.2012.FTu1B.1. URL: <https://www.osapublishing.org/abstract.cfm?URI=FiO-2012-FTu1B.1> (visited on 03/22/2021).
- [2] Andy Steinmann et al. “Generation of few-cycle pulses directly from a MHz-NOPA”. en. In: *Optics Express* 14.22 (2006), p. 10627. ISSN: 1094-4087. DOI: 10.1364/OE.14.010627. URL: <https://www.osapublishing.org/oe/abstract.cfm?uri=oe-14-22-10627> (visited on 03/26/2021).
- [3] Issa Tamer et al. “Few-cycle fs-pumped NOPA with passive ultrabroadband spectral shaping”. en. In: *Optics Express* 28.13 (June 2020), p. 19034. ISSN: 1094-4087. DOI: 10.1364/OE.388344. URL: <https://www.osapublishing.org/abstract.cfm?URI=oe-28-13-19034> (visited on 03/26/2021).
- [4] G. Cirimi et al. “Few-optical-cycle pulses in the near-IR from a non-collinear optical parametric amplifier”. In: *2007 European Conference on Lasers and Electro-Optics and the International Quantum Electronics Conference*. June 2007, pp. 1–1. DOI: 10.1109/CLEOE-IQEC.2007.4386300.
- [5] Giulio Cerullo and Sandro De Silvestri. “Ultrafast optical parametric amplifiers”. en. In: *Review of Scientific Instruments* 74.1 (Jan. 2003), pp. 1–18. ISSN: 0034-6748, 1089-7623. DOI: 10.1063/1.1523642. URL: <http://aip.scitation.org/doi/10.1063/1.1523642> (visited on 03/22/2021).
- [6] Ian N. Ross et al. “Analysis and optimization of optical parametric chirped pulse amplification”. en. In: *Journal of the Optical Society of America B* 19.12 (Dec. 2002), p. 2945. ISSN: 0740-3224, 1520-8540. DOI: 10.1364/JOSAB.19.002945. URL: <https://www.osapublishing.org/abstract.cfm?URI=josab-19-12-2945> (visited on 03/27/2021).
- [7] J. A. Armstrong et al. “Interactions between Light Waves in a Nonlinear Dielectric”. en. In: *Physical Review* 127.6 (Sept. 1962), pp. 1918–1939. ISSN: 0031-899X. DOI: 10.1103/PhysRev.127.1918. URL: <https://link.aps.org/doi/10.1103/PhysRev.127.1918> (visited on 03/22/2021).
- [8] D. N. Schimpf et al. “Theoretical analysis of the gain bandwidth for noncollinear parametric amplification of ultrafast pulses”. en. In: *Journal of the Optical Society of America B* 24.11 (Nov. 2007), p. 2837. ISSN: 0740-3224, 1520-8540. DOI: 10.1364/JOSAB.24.002837. URL: <https://www.osapublishing.org/abstract.cfm?URI=josab-24-11-2837> (visited on 03/22/2021).
- [9] K. Fujioka et al. “Partially deuterated potassium dihydrogen phosphate optimized for ultrabroadband optical parametric amplification”. en. In: *Journal of Applied Physics* 117.9 (Mar. 2015), p. 093103. ISSN: 0021-8979, 1089-7550. DOI: 10.1063/1.4913298. URL: <http://aip.scitation.org/doi/10.1063/1.4913298> (visited on 03/27/2021).
- [10] Ian Walmsley, Leon Waxer, and Christophe Dorrer. “The role of dispersion in ultrafast optics”. en. In: *Review of Scientific Instruments* 72.1 (Jan. 2001), pp. 1–29. ISSN: 0034-6748, 1089-7623. DOI: 10.1063/1.1330575. URL: <http://aip.scitation.org/doi/10.1063/1.1330575> (visited on 03/22/2021).

- [11] Ian A. Walmsley and Christophe Dorrer. “Characterization of ultrashort electromagnetic pulses”. en. In: *Advances in Optics and Photonics* 1.2 (Apr. 2009), p. 308. ISSN: 1943-8206. DOI: 10.1364/AOP.1.000308. URL: <https://www.osapublishing.org/aop/abstract.cfm?uri=aop-1-2-308> (visited on 04/30/2021).
- [12] Robert W. Boyd and Debbie Prato. *Nonlinear Optics*. San Diego, UNITED STATES: Elsevier Science & Technology, 2008. ISBN: 978-0-08-048596-6. URL: <http://ebookcentral.proquest.com/lib/rochester/detail.action?docID=404866> (visited on 03/26/2021).